



## Brief communication: Improving botanical monitoring in proglacial areas with high-resolution UAV data

César Deschamps-Berger<sup>1,2</sup>, Nahia Carretero Roque<sup>1</sup>, Jesús Revuelto<sup>1</sup>, Francisco Rojas-Heredia<sup>1</sup>, Ixeia Vidaller<sup>1</sup>, Aina Alvarez<sup>1</sup>, Alba López-Varela<sup>1</sup>, Olatz Fernández<sup>1</sup>, Sara Palacio<sup>1</sup>, Juan Ignacio Lopez-5 Moreno<sup>1</sup>, Pablo Tejero Ibarra<sup>1</sup>

<sup>1</sup> Pyrenean Institute of Ecology, Zaragoza, Spain

<sup>2</sup> GEODE, UMR, CNRS, University of Jean-Jaurès, Toulouse, France

10 *Correspondence to:* César Deschamps-Berger (cesar.deschamps-berger@univ-tlse2.fr)

**Abstract.** Proglacial areas are undergoing rapid ecological and land cover changes as glaciers retreat globally. Field campaigns are essential in proglacial environments to monitor the colonization of the deglaciated areas by the vegetation. In this study, we evaluate the benefit of using optical UAV images to optimize botanical data collection during these campaigns. We compared the vegetation cover measured in situ by experts with the vegetation cover derived from high-15 resolution UAV images in a high-mountain environment below the Aneto glacier in the Pyrenees. Retrieving the vegetation cover from UAV images provided valuable and complementary data to traditional in situ detailed observations.

### 1 Introduction

The vegetation is rapidly evolving in many places of the planet as a consequence of land cover changes and shifting climatic areas (Song et al., 2018). In temperate mountains, the vegetation distribution is largely affected by meteorological 20 conditions, snowpack distribution, local topography and soil properties, as well as human activities such as livestock grazing and intensification or abandonment of agricultural practices (García-Ruiz et al., 2011; Revuelto et al., 2022; Choler et al., 2025). The shrinkage of glaciers is also a driver of vegetation changes, as it uncovers bare areas prone to colonization by surrounding plants (Bosson et al., 2023; Ficetola et al., 2024). This phenomenon is common due to the widespread glacier mass losses in the context of temperature increase (Dussaillant et al., 2025).  
25 Vegetation colonization in proglacial areas has been studied through extensive in situ observation campaigns, which aim at understanding the type of plants leading the colonization and the pace of the process (e.g. Zimmer et al., 2018; Fischer et al., 2019). Vegetation cover, i.e. the proportion of the surface occupied by vegetation when observed from a top-down perspective, is a key indicator of the post-glacial colonization, as it equalled zero at the time of the ice retreat and tend to progressively increase thereafter (Bayle et al., 2023). However, in situ observations of the vegetation are only possible at a 30 few dozens of plots of, typically, 1 m<sup>2</sup> to 4 m<sup>2</sup> and are difficult to collect due to logistical constraints. The design of the



sampling strategy (i.e. number of samples, method of selection) aims at ensuring the statistical robustness of the signals measured. However, the representativity of the results may be uncertain due to the large numbers of variables to monitor, the discontinuous sampling and the small number of observations.

Mapping of the vegetation cover through remote sensing ensures a continuous sampling of an area often larger than what 35 field campaigns can cover. However, proglacial environments present specific challenges due to the vegetation scarcity and the complex topography. Images from Landsat satellites were used to derive long-term trends of the normalized difference vegetation index and of the vegetation cover taking advantage from the archive dating back to 1984 (Bayle et al., 2023, 2021; Fischer et al., 2019). Unmanned Aerial Vehicles (UAV) have emerged as a convenient solution for very high resolution mapping of complex terrain such as proglacial areas (Vidaller et al., 2024; Corte et al., 2024). Thus, UAV vegetation cover 40 maps have already been used at 12 cm resolution to calibrate the sensitivity of Landsat NDVI at 30 m to subpixel vegetation variability (Bayle et al., 2021). The vegetation cover was also derived from UAV images at 7 cm resolution in a proglacial area, but was not evaluated against reference measurements (Wei et al., 2021). Similarly, a land cover map was derived from UAV images at 4.5 cm resolution near the front of an Austrian glacier (Zangerl et al., 2022). The map was found to be accurate with an overall accuracy of 87%, but this evaluation was based on a set of reference values extracted from the UAV 45 images and not from an external, independent, reference dataset such as in situ observations.

Thus, there remains a knowledge gap regarding how the vegetation cover derived from high-resolution UAV images compares to the traditional expert in situ observations in recently deglaciated areas, which are at the base of most studies in the topic so far. Here, we aim at filling this gap and answering the following three questions: how do UAV vegetation cover estimates compare to in situ observations in a proglacial environment? What is the impact of the UAV product resolution on 50 the vegetation cover retrieval? How can UAV data be used to complete or improve in situ sampling strategies? We used in situ observation collected by botanist experts below the front of the Aneto glacier in the central Pyrenees and concurrent with images obtained by a UAV flight from which the vegetation cover was estimated. The comparison of both datasets enables to estimate the representativeness of the in situ sampling strategy, the accuracy of the UAV vegetation cover and the strengths and weaknesses of both methods.

55

## 2 Study site and methods

### 2.1 Study site

The Aneto glacier is the largest glacier of the Pyrenees with 34.4 ha in 2023 (Izagirre et al., 2024). The area covered by the 60 glaciers of the massif have decreased by 87% since their last maximal extent during the little ice age (LIA) circa 1850 (Vidaller et al., 2024). The glacier retreat revealed granitic rock later partially covered by detritic sediments, shallow soil and low vegetation (Vidaller et al., 2025). The area has an average slope of 22° between the frontal moraine and the current glacier location, facing the north-east. The climate is characterized by high-mountain conditions with a long lasting seasonal



snowpack and short growing season. The in situ observations have been collected at six sites, labelled A1 to A6, between the LIA moraine (2500 m a.s.l.) and the current extent of the glacier (3040 m a.s.l.) during two field campaigns in August 2023  
65 (A1-2-4-5-6) and 2024 (A3, Fig. 1). The UAV survey focused on two areas of interest, one centred on the points A1 and one including the points A4 to A6 (Fig. 1).

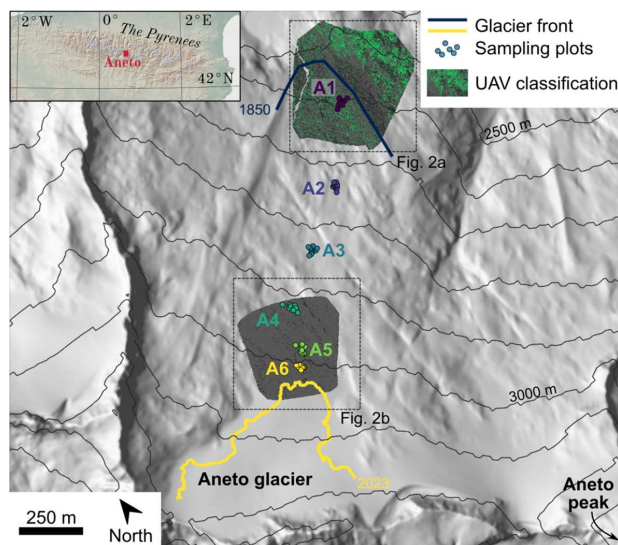


**Figure 1.** Study sites along the Aneto glacier retreat gradient (A1-A6). The vegetation cover was estimated from UAV images in the upper part (including A4, A5 and A6) and the lower part (A1) of the deglaciated area. Zoom on the land use cover map from UAV is provided in Fig. S1 and 3.

## 2.2 UAV surveys

The UAV surveys were conducted on 08 and 09 August 2023 with a Parrot ANAFI quadcopter UAV equipped with a RGB camera (21 Mp 1/2.4" CMOS sensor, 35 mm flens format equivalent). The images of each survey overlapped a minimum of  
75 70% transversally and 80% longitudinally, and each area was flown at 20 m and 70 m above the ground, which then were processed with Structure from motion (SfM) software to generate orthoimages. The higher resolution flights covered 0.3 ha (A1) and 1.3 ha (A4-A6), while the lower resolution flight covered 18.8 ha (A1) and 12.9 ha (A4-6). Additionally, nine plots of the site A1 and five plots of A6 were imaged by a nadir acquisition from a low static UAV flight at ~3 m above ground resulting in images with millimetric resolution.

80 Orthomosaic production was performed using PIX4D mapper (version 4.4.12) through SfM methods. The automatic processing began with internal and external calibrations of the camera parameters to compute the camera geometry, its



position and its orientation at the time of each pictures acquisition. Then, an automatic keypoint matching process identified common areas across at least two images to refine the internal and external camera calibration. A densified 3D point cloud was then generated, allowing the computation of a digital surface model and a mosaic of orthoimages (Revuelto et al., 2021).

85 All products were generated in the WGS 84 / UTM Zone 31N projection.

The UAV has the positioning standard error of a regular GPS. Thus, the geolocation accuracy of the initial orthomosaics was ~4 m and was further improved by manually identifying control points in the contemporary aerial images at 0.5 m spatial resolution from the Instituto Geografico Nacional through georeferencing facility in QGIS (QGIS Development Team). The low resolution images (70 m flight height) were georeferenced using a polynomial of degree three transform and further used

90 as reference to georeference the high-resolution images (30 m and 3 m flight height) with a linear transform. The mean residual of the georeferencing was of 0.68 m, 0.40 m and 0.04 m. Finally, the images were resampled at respectively 5 cm, 1 cm and 0.1 cm resolution, with a bilinear interpolation to homogenize the series of images of the two areas of interest. The parts covered by the glacier, water bodies and snow were manually masked. The images were then classified in a land cover map using a random forest classifier based on training samples divided into four classes (rock, rock in the shade, vegetation, 95 and vegetation in the shade), following the methodology implemented for satellite images in Deschamps-Berger et al. (2020), but solely using the red, green, and blue bands. This resulted in an ensemble of six sets of UAV derived land cover maps, based on the area (A1 or A4-6) and the resolution of the cover map (0.1 cm, 1 cm, 5 cm).

### 2.3 In situ vegetation surveys

In situ measurements were considered the ground truth for the vegetation cover. The vegetation cover was determined in 10

100 plots of 1 m by 1 m distributed around the point A1 to A6. The location of the plots were chosen to sample, above all, the diversity of species and was, thus, not specifically designed to map robustly the vegetation cover. Each plot was divided into 25 cells of 0.2 x 0.2 m, in which the proportion occupied by vegetation (including mosses), soil and rock were estimated by experienced observers. The detailed list of species encountered was also determined to define species abundance and plant 105 community composition along the elevation gradient, but was not used in this study.

105 2.4 Comparison of in situ and UAV vegetation cover

For each plot, an in situ vegetation cover value in percent was available. The vegetation cover was calculated from each UAV land cover map as the proportion of pixel classified as vegetation within a 1 m by 1 m square centred on the in situ sampling points located within the UAV images. Due to the varying coverage of the UAV acquisitions, 14, 12 and 38 points were available for comparison for the UAV resolution of 0.1 cm, 1 cm and 5 cm respectively. The agreement of the UAV and 110 in situ vegetation cover was estimated with the Pearson correlation between both datasets, and the mean and the standard deviation of the residuals (UAV minus in situ). The representativeness of the in situ sampling was evaluated by comparing the UAV vegetation cover at the plots location and over the whole elevation band to which they belonged. Finally, the



gradients in vegetation cover with elevation measured by UAV and in situ observations were calculated as a linear fit through the median of the vegetation cover at each elevation.

115 **3 Results**

**3.1 Vegetation cover maps from UAV images**

The maps derived from UAV images highlighted the expected reduction in vegetation cover between the low-elevation and high-elevation sites (Fig. S1). They also showed the large spatial variability of the vegetation cover around the point A1,

associated to a patchy pattern. The moraine appeared as clear discontinuity with low vegetation cover separating two areas  
120 with higher vegetation cover. Around the point A4-6, the vegetation appeared much sparser in the 1 cm and 5 cm maps.

Individual pixels were identified as vegetated in an unrealistic pattern, likely as a result of misclassification of shades or coloured rock. However, individual large plants with a radius of 10 cm or greater were properly identified (Fig. S2). Some of these were present in the 1 cm map and not in the 5 cm one. Overall, pixels likely wrongly classified as vegetated appeared at the border of shaded areas and within them, suggesting the difficulty to classify mixed pixels and pixels with low contrast.

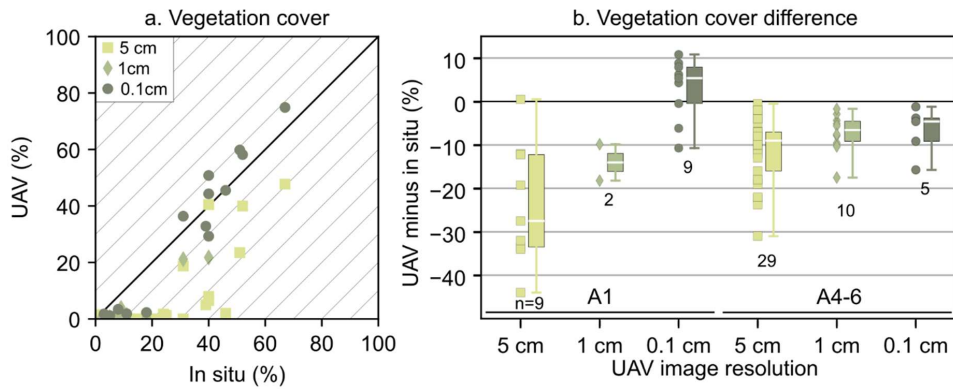
125 **3.2 Comparison of vegetation cover estimates by UAV versus in situ surveys**

The level of agreement between in situ observation and UAV derived vegetation cover was found to vary with the site and the resolution considered, with better results for A1 plots compared to A4-6 (Fig. 2 and 3, Table S1). For A1 plots, UAV vegetation cover was lower on average for 5 cm spatial resolution UAV map estimates compared to in situ values (-23.8%).

The agreement of the 0.1 cm spatial resolution UAV map was better with a mean bias of only +2.9%. Only two plots were  
130 available in the 1 cm map, which did not allow for robust statistical calculations. The variability of the vegetation cover was

well captured in the maps at 5 cm and 0.1 cm with a Pearson correlation coefficient of 0.60 and 0.88, respectively. The standard deviation of the residuals (UAV minus in situ) was 13.2% and 6.8% for 5 cm and 0.1 cm maps, respectively, which is remarkably lower than the in situ vegetation cover values, which ranged from 31% to 67% (Fig 2, Table S1). The

differences between UAV and in situ data were relatively larger for plots A4-6, where the mean bias of the residuals ranged  
135 from -6.9% (0.1 cm) to -11.1% (5 cm), which is close to the mean vegetation cover of 11.1%. The standard deviation of the residuals was similarly larger for the 5 cm map (7.3%) than for the 1 cm map (4.3%) and the 0.1 cm map (5.1%), although the smaller sample size for the latter should be noted (N=5).



140 **Figure 2.** Scatter plot of the vegetation cover measured by classification of UAV images and by in situ observation (a).  
 Difference of vegetation cover broken down by UAV image resolution (b). The UAV values are extracted from a 2 m by 2 m square centred on the in situ sampling location.

### 3.3 Vegetation cover gradient with elevation

Despite the general underestimation of the UAV vegetation cover compared to the in situ one, the decrease in vegetation  
 145 cover between low areas (median cover of 12.3% at 2450–2500 m a.s.l.) and high areas (median of 0% from 2900 m a.s.l.) is  
 identified in UAV vegetation cover estimates (Fig. 3a). The exact gradient of decrease of the vegetation cover with elevation  
 is variable between the UAV products and the in situ observation. Thus, between the 2600 m – 2650 m and 2950 m – 3000 m  
 bands for which all products are available, the vegetation cover decrease by only -3% per 100 m elevation for the 5 cm  
 vegetation cover product, but by -8%, -12% and -9% per 100 m for, respectively, the 1 cm, the 0.1 cm and the in situ  
 150 products, respectively.

The larger area covered by the UAV flight also enabled us to expand the observation to areas out of the frontal moraine  
 contour, which were not observed in situ (Fig. 3b). This showed that the vegetation cover is much higher under 2450 m a.s.l.,  
 marking a discontinuity with areas above. At an altitude where the moraine marks the past glacier presence, the vegetation  
 cover is higher out of the moraine than within the moraine up to 2550 m a.s.l. and similar on both sides of the moraine  
 155 above. Thus, the past presence of a glacier did not result in a systematic difference of vegetation and other variables must  
 explain such cover variation within a narrow 250 m band of elevation (2400 m a.s.l. to 2650 m a.s.l.).

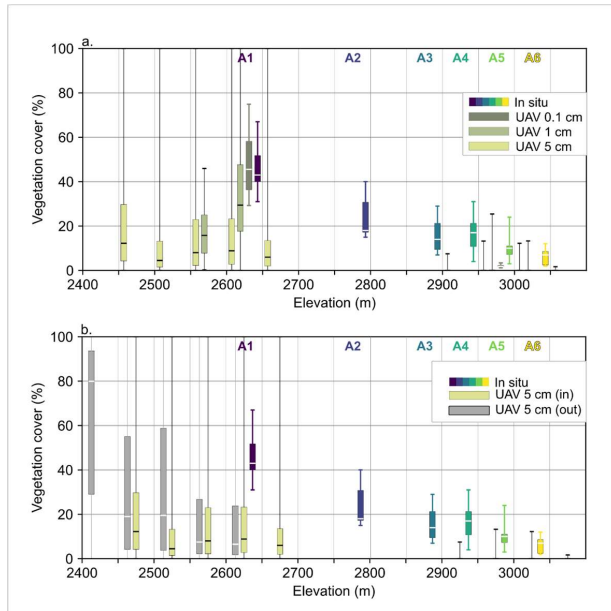


**Figure 3.** Distribution of the vegetation cover derived from UAV 5 cm, 1 cm and 0.1 cm images within the moraine extent and from in situ observation at the sampling points A1 to A6 (a). Distribution of the vegetation cover derived from UAV 5 cm images within the moraine extent (i.e. once ice-covered during the LIA) in green, out of the moraine extent (i.e. not ice-covered even during the LIA) in grey and from in situ observation at the sampling points A1 to A6 (b).

### 3.4 Evaluation of the in situ sampling strategy

The distribution of the 5 cm UAV vegetation cover is generally comparable whether it is sampled at the in situ plots location 165 or over the whole elevation band (Fig. S3). However, the in situ sampling does not sample the maximal values of the area and the median of the in situ sampling (19 %) is higher than the median of the complete distribution (12 %). This suggests a bias in the in situ sampling strategy, which leads to an overestimation of the median value and an underestimation of the variability. Such assessment is not possible for the higher area (A4-A6) due to the distribution of vegetation cover being overwhelmingly dominated by values close to zero.



170 **4 Discussion**

We found that UAV-derived vegetation cover estimates matched reasonably well with in situ measurements in proglacial environments, since they were able to capture the vegetation cover decrease from low to high elevation. Similarly, random forest classifier was previously found to properly identify vegetation classes in a mediterranean, alpine and proglacial environments on 1 cm to 6 cm UAV images (Zangerl et al., 2022; Niederheiser et al., 2021; Gonçalves et al., 2016). The 175 systematic underestimation of the vegetation cover found here is similar in magnitude to biases found in similar UAV derived cover estimates, although in a varying direction (Chen et al., 2016; Niederheiser et al., 2021). More complex vegetation cover retrievals using convolutional neural networks or adding bands derived from RGB images and topographic information do not seem to guarantee better results (Niederheiser et al., 2021; Zangerl et al., 2022). However, it might be 180 beneficial to acquire near-infrared images to derive the NDVI values, as it is an index specific to vegetation (Bayle et al., 2021).

The UAV retrievals captured fairly well the variability between plots with high vegetation cover (i.e. from low altitude), but not those where vegetation was really sparse (i.e. at high altitude). The increase in the resolution of the UAV vegetation cover map improved the agreement with in situ measurements with a reduction of the absolute bias from -23.8% (5 cm) to 185 2.90% (0.1 cm) in areas where the cover was high. Similarly, the bias also decreased with increased resolution in areas with sparse vegetation. However, in such areas, the mean bias for 0.1 cm images was -6.9%, which remained high relative to the mean vegetation cover value which was 9.0%. These 0.1 cm high-resolution images were acquired in static mode and could only be acquired over small areas. We found that the gradient of vegetation cover with elevation was not necessarily 190 impacted by these biases as they were consistent at all elevations. Thus, the decrease in vegetation cover was similar for 1 cm, 0.1 cm product and the in situ observation, ranging from 8% to 12% of reduction per 100 m elevation. Only the gradient derived from the 5 cm UAV product strongly underestimated the in situ gradient with a 3% reduction per 100 m, probably due to the bias being larger than the vegetation cover at high elevation.

A good compromise between the area covered and the accuracy of the vegetation cover estimate could be achieved with 195 UAV images with a spatial resolution of 1 cm to 5 cm, corrected with a few in situ vegetation cover measurements or a few higher resolution images. Furthermore, more accurate vegetation cover over larger areas could be expected with better sensors. The UAV of this study was chosen due to its low weight, but at the cost of a medium resolution of 20 megapixels. Sensors with 50 to 100 megapixels are becoming increasingly available and would increase the area covered in this study at a given resolution.

The poor quality of the UAV retrievals over low vegetation cover could be due to the spatial distribution of the vegetation in 200 these areas or to a mismatch between the in situ observer and the classification definition of vegetation. In these plots, the vegetation is gathered in a few patches and is sometimes composed of herbaceous plants, which results in a larger proportion of mixed pixels composed of vegetation and rocks (Fig. S2). The binary classification used here is probably not adapted to



these pixels. In order to avoid adding endlessly new categories (i.e., mixed pixels), the fractional vegetation cover could be directly calculated at the pixel scale (Chen et al., 2016) using a regression algorithm such as random forest regressor or gradient boosting. These are hard to classify and can lead to an underestimation of the vegetation cover. However, UAV 205 images in such sparse vegetation environments can be used to detect large isolated plants of typically 30 cm radius over large areas and complex topography, which would be time-consuming and dangerous for an observer to explore. For instance, 18 groups of pixels larger than a circle with a radius of 10 cm and classified as vegetation were automatically extracted from the 1.3 ha covered by the high-resolution map in the high-elevation area, which is the most difficult to explore due to its relief (not shown). Such vegetation cover mapping could be a first preparatory step to guide an observer in the field. At the current 210 stage of development of UAV methodologies for vegetation survey, the level of detail with the highest resolution images does not enable to determine the exact species of plants present, similarly to what was observed in the proglacial area of a glacier in the Tianshan Mountains (Fig. S2 in Wei et al., 2021). Thus, expert determination with direct observations of the vegetation remains necessary to determine precisely the plant communities.

A clear benefit from UAV vegetation cover maps is the larger area covered, which informs about the general context of the 215 study site. For instance, the 5 cm images at low elevation covered about 0.2 km<sup>2</sup> inside and outside the frontal moraine encompassing all the A1 in situ sampling points. This large coverage enabled to expand observations to areas not monitored in situ and to highlight the similarity between vegetation on both sides of the moraine above 2550 m a.s.l. (Fig. 3). The continuous cover of the UAV maps also enabled to verify the representativeness of the sampling strategy by comparing the vegetation cover distribution to the one of the corresponding altitude band (Fig. S1 and 6). A slight positive bias in the in situ 220 sampling strategy was, thus, likely identified leading to an overestimation of the true vegetation cover distribution. This difference was found to be satisfactory given that the sampling strategy was optimized to sample the species diversity.

## 5 Conclusion

We highlighted the benefits of the UAV vegetation cover surveys which are their ability to cover large area in complex 225 terrain and to determine accurately the spatial variability of the vegetation cover between contrasted elevation or within a given area if the cover is sufficiently high (i.e. low elevation). However, UAV vegetation cover showed clear bias compared to in situ observations leading to a general underestimation of the cover. This bias is reduced with higher resolution images but at the cost of a reduced area covered. Additional benefits from UAV mapping are the ability to evaluate the in situ sampling strategy. Future work should aim at designing the optimal UAV flight configurations (elevation, camera 230 adjustments) to satisfy the image resolution requirements and the coverage of the area relevant to investigate vegetation colonization in proglacial environments. We conclude that UAV are a reliable tool to complement in situ observation of the vegetation cover, although they cannot replace detailed in situ inventories to retrieve the vegetation community composition and diversity.



#### Code and data availability

235 Code: [https://framagit.org/cesardb/aneto\\_glacier\\_vegetation/-/tree/publication\\_UAV\\_article](https://framagit.org/cesardb/aneto_glacier_vegetation/-/tree/publication_UAV_article)  
Data: <https://doi.org/10.5281/zenodo.17989880>

#### Author contributions

*CDB, JR, JILM and PTI* conceived the ideas and designed methodology; all authors collected the data; *NCR, AA, ALV* and *PTI* analysed the botanical data; *CDB* analysed the UAV data *CDB* led the writing of the manuscript. All authors contributed  
240 critically to the drafts and gave final approval for publication.

#### Competing interests

The authors declare no competing interest.

#### Disclaimer

245 Copernicus Publications remains neutral with regard to jurisdictional claims made in the text, published maps, institutional affiliations, or any other geographical representation in this paper. While Copernicus Publications makes every effort to include appropriate place names, the final responsibility lies with the authors. Views expressed in the text are those of the authors and do not necessarily reflect the views of the publisher.

#### Acknowledgements

We thank the authorities of the Posets-Maladeta Natural Park for facilitating our campaigns.

#### 250 Financial support

This study was supported by the POCTEFA program from the EU through FLORAPYR 3D (EFA064/01) project, the Spanish Ministry of Science and Innovation through MARGISNOW (PID2021-124220OB-100) project and postdoctoral grant (FJC2021-047268-I), the Leonardo program of the BBVA research foundation through MeltingIce project and the French Space Agency (Centre National d'Etudes Spatiales, CNES) postdoctoral fellowship. Jaca Herbarium has allocated its  
255 own resources to the study.



### Review statement

The review statement will be added by Copernicus Publications listing the handling editor as well as all contributing referees according to their status anonymous or identified.

### 260 References

Bayle, A., Roussel, E., Carlson, B. Z., Vautier, F., Brossard, C., Fovet, E., et al.: Sensitivity of Landsat NDVI to subpixel vegetation and topographic components in glacier forefields: assessment from high-resolution multispectral UAV imagery. *Journal of Applied Remote Sensing*, 15(04), <https://doi.org/10.1117/1.JRS.15.044508>, 2021.

265 Bayle, A., Carlson, B. Z., Zimmer, A., Vallée, S., Rabatel, A., Cremonese, E., et al.: Local environmental context drives heterogeneity of early succession dynamics in alpine glacier forefields. *Biogeosciences*, 20(8), 1649–1669, <https://doi.org/10.5194/bg-20-1649-2023>, 2023.

Bosson, J. B., Huss, M., Cauvy-Fraunié, S., Clément, J. C., Costes, G., Fischer, M., et al.: Future emergence of new ecosystems caused by glacial retreat. *Nature*, 620(7974), 562–569. <https://doi.org/10.1038/s41586-023-06302-2>, 2023.

270 Chen, J., Yi, S., Qin, Y., and Wang, X.: Improving estimates of fractional vegetation cover based on UAV in alpine grassland on the Qinghai–Tibetan Plateau. *International Journal of Remote Sensing*, 37(8), 1922–1936, <https://doi.org/10.1080/01431161.2016.1165884>, 2016.

Choler, P., Bonfanti, N., Reverdy, A. et al. Legacy of snow cover on alpine landscapes. *Communications Earth & Environment*, 6, 758: <https://doi.org/10.1038/s43247-025-02702-6>, 2025.

275 Corte, E., Ajmar, A., Camporeale, C., Cina, A., Coviello, V., Giulio Tonolo, F., Godio, A., Macelloni, M. M., Tamea, S., and Vergnano, A.: Multitemporal characterization of a proglacial system: a multidisciplinary approach, *Earth Syst. Sci. Data*, 16, 3283–3306, <https://doi.org/10.5194/essd-16-3283-2024>, 2024.

Dussaillant, I., Hugonnet, R., Huss, M., Berthier, E., Bannwart, J., Paul, F., and Zemp, M.: Annual mass change of the world's glaciers from 1976 to 2024 by temporal downscaling of satellite data with in situ observations. *Earth System Science Data*, 17(5), 1977–2006. <https://doi.org/10.5194/essd-17-1977-2025>, 2025.

280 Ficetola, G. F., Marta, S., Guerrieri, A., Cantera, I., Bonin, A., Cauvy-Fraunié, S., et al.: The development of terrestrial ecosystems emerging after glacier retreat. *Nature*, 632(8024), 336–342. <https://doi.org/10.1038/s41586-024-07778-2>, 2024.

Fischer, A., Fickert, T., Schwaizer, G., Patzelt, G., and Groß, G.: Vegetation dynamics in Alpine glacier forelands tackled from space. *Scientific Reports*, 1–13, <https://doi.org/10.1038/s41598-019-50273-2>, 2019.

285 Gonçalves, J., Henriques, R., Alves, P., Sousa-Silva, R., Monteiro, A. T., Lomba, Â., et al.: Evaluating an unmanned aerial vehicle-based approach for assessing habitat extent and condition in fine-scale early successional mountain mosaics. *Applied Vegetation Science*, 19(1), 132–146. <https://doi.org/10.1111/avsc.12204>, 2016.



Izagirre, E., Revuelto, J., Vidaller, I., Deschamps-Berger, C., Rojas-Heredia, F., Rico, I., et al.: Pyrenean glaciers are disappearing fast: state of the glaciers after the extreme mass losses in 2022 and 2023. *Regional Environmental Change*, 24(4), 172, <https://doi.org/10.1007/s10113-024-02333-1>, 2024.

290 Niederheiser, R., Winkler, M., Di Cecco, V., Erschbamer, B., Fernández, R., Geitner, C., et al.: Using automated vegetation cover estimation from close-range photogrammetric point clouds to compare vegetation location properties in mountain terrain. *GIScience & Remote Sensing*, 58(1), 120–137. <https://doi.org/10.1080/15481603.2020.1859264>, 2021.

QGIS Development Team, 2025. QGIS Geographic Information System. Open Source Geospatial Foundation Project. <http://qgis.osgeo.org>, 2021.

295 Revuelto, J., López-Moreno, J. I., & Alonso-González, E.: Light and Shadow in Mapping Alpine Snowpack With Unmanned Aerial Vehicles in the Absence of Ground Control Points. *Water Resources Research*, 57(6), e2020WR028980. <https://doi.org/10.1029/2020WR028980>, 2021.

Revuelto, J., Gómez, D., Alonso-González, E. et al.: Intermediate snowpack melt-out dates guarantee the highest seasonal grasslands greening in the Pyrenees. *Scientific Report*, 12, 18328: <https://doi.org/10.1038/s41598-022-22391-x>, 2022.

300 Song, X.-P., Hansen, M. C., Stehman, S. V., Potapov, P. V., Tyukavina, A., Vermote, E. F., & Townshend, J. R.: Global land change from 1982 to 2016. *Nature*, 560(7720), 639–643. <https://doi.org/10.1038/s41586-018-0411-9>, 2018.

Vidaller, I., Moreno, A., Izagirre, E., Belmonte-Ribas, Á., Carcavilla, L., and López-Moreno, J. I.: Geomorphology of the Maladeta massif (Central Pyrenees): the traces of the last remaining glaciers. *Journal of Maps*, 20(1), 2347896, <https://doi.org/10.1080/17445647.2024.2347896>, 2024.

305 Vidaller, I., Otero, X. L., Igual, J. M., Nobrega, G. N., Ferreira, T. O., Moreno, A., and López-Moreno, J. I.: Incipient soils: New habitats in proglacial areas of the Maladeta massif (Central Pyrenees). *Science of The Total Environment*, 967, 178740. <https://doi.org/10.1016/j.scitotenv.2025.178740>, 2025.

Wei, T., Shangguan, D., Yi, S., and Ding, Y.: Characteristics and controls of vegetation and diversity changes monitored with an unmanned aerial vehicle (UAV) in the foreland of the Urumqi Glacier No. 1, Tianshan, China. *Science of The Total Environment*, 771, 145433. <https://doi.org/10.1016/j.scitotenv.2021.145433>, 2021.

310 Zangerl, U., Haselberger, S., and Kraushaar, S.: Classifying Sparse Vegetation in a Proglacial Valley Using UAV Imagery and Random Forest Algorithm. *Remote Sensing*, 14(19), 4919. <https://doi.org/10.3390/rs14194919>, 2022.

Zimmer, A., Meneses, R. I., Rabatel, A., Soruco, A., Dangles, O., and Anthelme, F.: Time lag between glacial retreat and upward migration alters tropical alpine communities. *Perspectives in Plant Ecology, Evolution and Systematics*, 30, 89–102.

315 <https://doi.org/10.1016/j.ppees.2017.05.003>, 2018.